

Slow Light Enhanced Silicon Chip Based Chem-Bio Sensors

Swapnajit Chakravarty¹, Xiaochuan Xu¹, Hai Yan², Wei-Cheng Lai², Yi Zou², Ray T. Chen^{1,2}

¹Omega Optics Inc., 8500 Shoal Creek Blvd., Bldg. 4, Suite 200, Austin, TX 78757

²Microelectronics Research Center, University of Texas, Austin, 10100 Burnet Road, Bldg. 160, Austin, TX 78758

swapnajit.chakravarty@omegaoptics.com, chenrt@austin.utexas.edu

Abstract: Silicon nanophotonic waveguides and microcavities are experimentally investigated. High density lab on chip sensor integration and high sensitivity sensors enabled by engineering slow light and analyte overlap integrals are demonstrated for chemical and biosensing applications.

OCIS codes: (230.5298) Photonic crystals, (230.5750) Resonators, (280.4788) Optical sensing and sensors.

1. Introduction

Silicon has been the material of choice of the photonics industry over the last decade due to its easy integration with silicon electronics as well as its optical transparency in the near-infrared and mid-infrared wavelengths. While considerations of micro- and nano-fabrication induced device parameter deviations and a higher than desirable propagation loss still serves as a bottleneck in many data communication applications on chip, applications as sensors do not require similar stringent controls. In recent years thus, photonic devices on chips are increasingly being demonstrated for chemical and biological sensing with performance metrics rivaling benchtop instruments and thus promising the potential of portable, handheld and wearable monitoring of various chemical and biological analytes. During the past decade, numerous silicon photonic components such as ring resonators [1], one-dimensional (1-D) and two-dimensional (2-D) photonic crystal (PC) waveguides and microcavities [2-4], Mach-Zehnder interferometers [5], sub-wavelength resonators and gratings [6] have been demonstrated experimentally as chemical and biological sensors. In this context, we note that another integrated photonics component, namely surface plasmon devices [7], despite plasmonic losses significantly higher than dielectric waveguide losses, have been commercialized as biosensors. However, planar integration and CMOS friendly fabrication, the ability to slowdown light as well as increase optical mode overlap with the analyte, offers silicon photonics several advantages plasmonic platforms.

In this paper, we will review our work in silicon nanophotonics with photonic crystal devices and sub-wavelength devices that enable slow light enhancement as well as enhancements in optical modal overlap, and their applications as high throughput, multiplexed, selective/ specific chemical and biological sensors.

2. Silicon Nanophotonic Microcavities for Biosensing

Photonic crystals (PCs) generated significant interest over the last decade because of their ability to confine light to ultra-small mode volumes in photonic crystal microcavities. Photonic crystal waveguides (PCWs) also demonstrated the ability to slow down the velocity of light as it propagates down a silicon waveguide with group index $n_g \sim 100$.

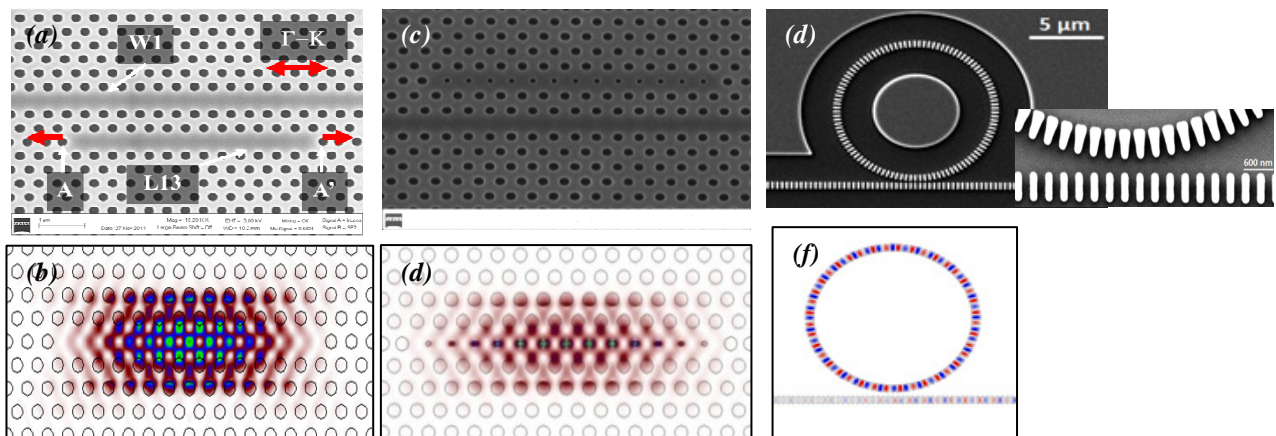


Fig. 1. (a) Scanning electron micrograph (SEM) of L13 PC microcavity coupled to W1 PC waveguide. The edge air holes are indicated by A and A' and the direction of shift indicated by the red arrows. (b) Resonance mode profile of L13 PC microcavity. (c) SEM image of L13 PC microcavity with defect holes (c) mode profile of the confined defect mode in (b). (e) SEM images of typical 5 μm SWGR with (a) trapezoidal silicon pillars. (inset) High magnification SEM image of a typical coupler of a 5 μm SWGR with trapezoidal pillars. (f) Typical top-view of the optical field in a SWGR on resonance.

Fig. 1(a) shows the scanning electron micrograph (SEM) of a typical PC microcavity in silicon, a L13 PC microcavity comprising 13 missing holes in a hexagonal lattice of air holes in silicon [3]. Fig. 1(b) shows the electric field intensity profile of the corresponding confined optical mode. Fig. 1(c) shows the SEM of the L13 PC microcavity with nanoholes at the center of the L13 PC microcavity and the corresponding field intensity profile in Fig. 1(d) [4]. In contrast to L13 PC microcavities, with $\sim 10\%$ optical mode overlap with the air holes surrounding the PC microcavity, with the incorporation of nanoholes, the confined optical mode is maximally confined in the nanoholes at the center of the L13 PC microcavity with a resultant overlap integral that can be as high as 20%. Since the analyte infiltrates the air holes, a larger analyte overlap integral results in a higher sensitivity to analyte concentrations. Various biosensing experiments done by our group showed that compared to 10 picomolar (pM) concentrations of avidin detected by biotin functionalized L13 PC microcavity surfaces, the L13 PC microcavity with nanoholes were able to detect 1 femto-molar (fM) concentration.

Recently, we demonstrated sub-wavelength ring resonators (SWGRR) as another promising nanophotonic microcavity for high sensitivity biosensing (Fig. 1(e)) [6]. The overlap integral in this case increases with decrease of silicon duty cycle and width of pillars, as shown in the inset of Fig. 1(e), meaning light confinement in the core is decreased and thus sensitivity is enhanced. However, optical loss will increase significantly. The resonant mode profile for a SWGRR is shown in Fig. 1(f). The calculated overlap 39.7% of quasi-transverse magnetic (TM) modes is larger than 30.2% of quasi-transverse electric (TE) modes with the same size pillar. In contrast to $\sim 120\text{nm}/\text{RIU}$ bulk sensitivities in PC microcavities, SWGRR microcavities showed $\sim 429\text{nm}/\text{RIU}$ bulk sensitivities. In both PC and SWGRR microcavities, as the photonic modes approach the light line of the cladding materials, they are subject to more radiation loss. Hence an appropriate design must consider the tradeoff between sensitivity and optical loss.

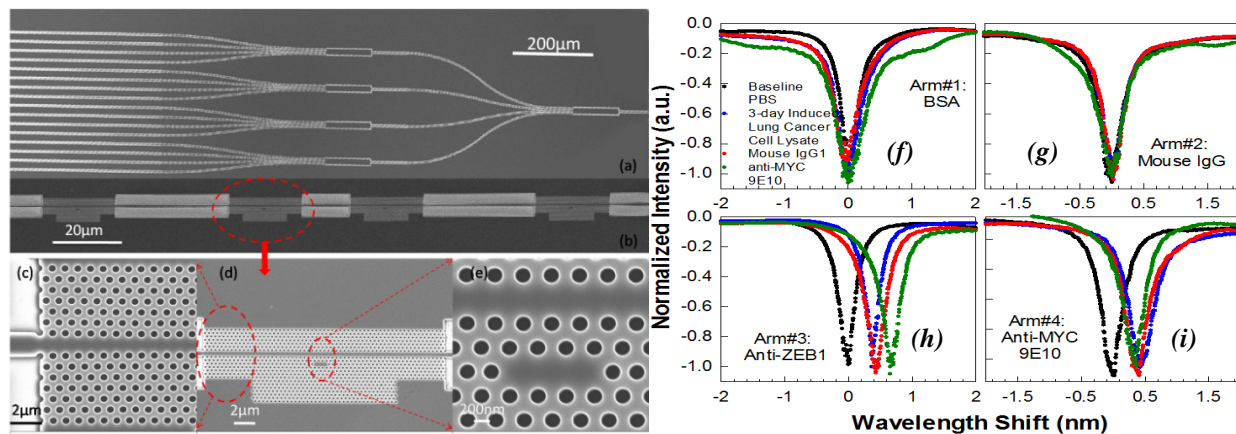


Fig. 2. (a) SEM of fabricated device [8] a) full device with 16 arms, b) each of the 16 arms with 4 cascaded microcavities, c) PCW adiabatic group index taper achieved by adiabatic width taper of PCW and high group index region, d) one of the 4 cascaded microcavities shown in (b), e) close up of the L3 PC microcavity located 2 rows away from a W1 PCW. (f) Multiplexed simultaneous specific detection of ZEB1 in lung cancer cell lysates with four arms of the MMI derivatized [4] with (a) bovine serum albumin (b) isotype matched control mouse IgG1 (c) anti-ZEB1 antibody and (d) anti-MYC 9E10 antibody. Baseline spectra for each arm is shown in black. Resonance wavelength positions shown in red, blue, green respectively with sequential addition of 3-day induced (1:10) lung cancer cell lysates, mouse IgG1 and anti-MYC 9E10, respectively.

Various designs of PC microcavities have been proposed for chemical and biosensing using microcavities with small mode volumes. The high sensitivity of PCs to changes in refractive index of the ambient promises the potential of creating high-density microarrays. As shown in Fig. 2, we experimentally demonstrated that PC microcavities can be integrated in series and parallel thereby enabling the simultaneous operation of a 64 sensor array integrating 4 PC microcavities in series each on 16 parallel waveguides on the output of a multimode interference (MMI) power splitter [8]. Such high density integration is significant in biosensing since several PC microcavities can be functionalized with the same probe biomarkers and others can be functionalized with corresponding negative and positive controls, so that measurements reduce false errors via redundancy, and at the same time ensure detection specificity within the same minuscule sample volume on chip. We experimentally demonstrated the concept in our detection of lung cancer cell line lysates with specificity using multiplexed photonic crystal cavities on chip [4]. The effective patient sample requirement can thus reduce from $64 \times 60 \mu\text{l} = 3,840 \mu\text{l}$ to only $60 \mu\text{l}$. Both these features are extremely critical in cancer research due to the paucity of real patient samples for testing. Added to this is the advantage of label-free operation so that end user biochemists can safely ignore issues caused by steric hindrance of labels in conventional design of fluorescent labeled biomarkers.

3. Slotted Photonic Crystal Waveguides: On-Chip Absorbance Sensors

Chemicals are best recognized by their unique wavelength specific optical absorption signatures. Slow light in photonic crystal slot waveguides (PCSW) [9] was used to reduce the optical absorption path length and achieve high detection sensitivity in on-chip optical absorption spectroscopy for selective detection of volatile organic compounds and greenhouse gases based on unique analyte absorption signatures in the near-infrared (near-IR) (Fig. 3). The principle of infrared absorption spectroscopy is based on the Beer-Lambert law. Transmitted intensity I is given by:

$$I = I_0 \exp(-\gamma\alpha L) \dots\dots\dots(1)$$

where I_0 is the incident intensity, α is the absorption coefficient of the medium, L is interaction length and γ is the medium-specific absorption factor determined by dispersion enhanced light-matter interaction. In conventional free-space systems, $\gamma = 1$; thus L must be large to achieve a suitable sensitivity of measured I/I_0 . For lab-on-chip systems, L must be small, hence γ must be large. Using perturbation theory,

$$\gamma = f \times \frac{c/n}{v_g} \dots\dots\dots(2)$$

where c = velocity of light in free space, v_g = group velocity in medium of effective index n and f = filling factor denoting relative fraction of optical field residing in the analyte medium. Equation 2 shows that slow light propagation (small v_g) significantly enhances absorption. Furthermore, greater the electric field overlap with analyte, greater the effective absorption by the medium. Both conditions of small v_g and high f are fulfilled in a PCSW.

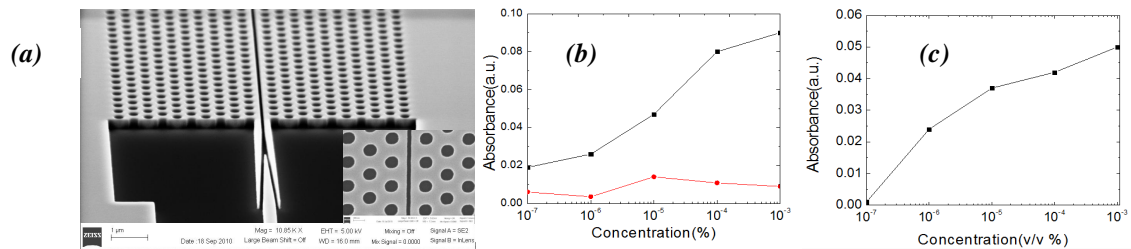


Fig. 3. (a) Scanning electron micrograph (SEM) image of fabricated PCSW. (inset) shows magnified top view of pattern. b) Absorbance of xylene measured at 1674nm with PC waveguide (in Black) and strip waveguide (in Red) c) Absorbance of TCE measured at 1644nm [9].

Absorption cross-sections of molecules in mid-infrared (mid-IR) are at least 2 orders of magnitude greater than their corresponding absorbance cross-sections in near-IR. In the mid-IR, we detected 10ppm (parts per million) triethylphosphate, a chemical warfare simulant with absorption cross-section $\sim 4 \times 10^{-19} \text{ cm}^2/\text{molecule}$, with only a 800 μm long PCSW [10] with detection limit 1ppm, at the wavelength of 3.4 μm in a silicon-on-sapphire platform.

4. Summary

Silicon nanophotonic sensors hold tremendous promise in chemical and biological sensing. Together with the maturity of room temperature lasers and detectors in the near-IR and mid-IR, nanophotonic sensors will enable handheld monolithic sensor devices in diverse applications in the near future. The research has been supported by SBIR awards from NSF #IIP-1127251, NIH/NCI # HHSN261201200043C, Army # W911SR-12-C-0046.

5. References

- [1] M. Iqbal, M.A. Gleeson, et al., "Label-Free Biosensor Arrays based on silicon ring resonators and high-speed optical scanning instrumentation", IEEE J. Sel. Top. Quant. Electron. 16(3), 654 (2010).
- [2] C. Kang, C.T. Phare, et al., "Photonic crystal slab sensor with enhanced surface area", Opt. Express 18(26), 27930 (2010).
- [3] S. Chakravarty, A. Hosseini, X. Xu, L. Zhu, Y. Zou, R. T. Chen, "Analysis of ultra-high sensitivity configuration in chip-integrated photonic crystal microcavity bio-sensors," Appl. Phys. Lett. 104, 191109 (2014)
- [4] S. Chakravarty, W-C. Lai, et al., "Multiplexed Specific Label-Free Detection of NCI-H358 Lung Cancer Cell Line Lysates with Silicon Based Photonic Crystal Microcavity Biosensors", Biosens. Bioelectron. 43, 50 (2013).
- [5] A. Densmore, M. Vachon, et al., "Silicon photonic wire biosensor array for multiplexed real-time and label-free molecular detection", Opt. Lett. 34(23), 3598 (2009).
- [6] H. Yan, L.Huang, et al., "Unique surface sensing property and enhanced sensitivity in microring resonator biosensors based on subwavelength grating waveguides," Opt. Express 24, 29724 (2016)
- [7] H. Sipova, S. Zhang, A.M. Dudley, D. Galas, K. Wang, and J. Homola, "Surface plasmon resonance biosensor for rapid label-free detection of microribonucleic acid at subfemtomole level", Anal. Chem. 82, 10110 (2010).
- [8] Y. Zou, S. Chakravarty, L. Zhu, and R. T. Chen, "The role of group index engineering in series-connected photonic crystal microcavities for high density sensor microarrays" Appl. Phys. Lett. 104, 141103 (2014).
- [9] W-C. Lai, S Chakravarty, Y Zou, and RT Chen, "Multiplexed detection of xylene and trichloroethylene in water by photonic crystal absorption spectroscopy", Optics Lett. 38 (19), 3799 (2013)
- [10] Y. Zou, S. Chakravarty, P. Wray, and R. T. Chen, "Mid-Infrared Holey and Slotted Photonic Crystal Waveguides in Silicon-on-Sapphire for Chemical Warfare Simulant Detection," Sensors and Actuators B 221, 1094 (2015).